Title

An experimental investigation of design parameters for pico-hydro Turgo turbines using a response surface methodology

Journal

Renewable Energy, 85(C)

ISSN

0960-1481

Authors

Gaiser, Kyle
Erickson, Paul
Stroeve, Pieter
et al.

Publication Date

2016

DOI

10.1016/j.renene.2015.06.049

Peer reviewed

Renewable Energy 85 (2016) 406–418

Contents lists available at ScienceDirect

Renewable Energy

journal homepage: www.elsevier.com/locate/renene

An experimental investigation of design parameters for pico-hydro Turgo turbines using a response surface methodology

Kyle Gaiser [a, c], Paul Erickson [a, *], Pieter Stroeve [b], Jean-Pierre Delplanque [a]

[a] University of California Davis, Department of Mechanical and Aerospace Engineering, One Shields Avenue, Davis, CA 95616, USA
[b] University of California Davis, Department of Chemical Engineering, One Shields Avenue, Davis, CA 95616, USA
[c] Sandia National Lab, Livermore, CA, USA

ARTICLE INFO

Article history:
Received 9 February 2015
Received in revised form
3 June 2015
Accepted 17 June 2015
Available online xxx

Keywords:
Pico-hydro
Turgo turbine
Hydroelectricity
Optimization
Central composite design
Response surface methodology

ABSTRACT

Millions of off-grid homes in remote areas around the world have access to pico-hydro (5 kW or less) resources that are undeveloped due to prohibitive installed costs ($/kW). The Turgo turbine, a hydroelectric impulse turbine generally suited for medium to high head applications, has gained renewed attention in research due to its potential applicability to such sites. Nevertheless, published literature about the Turgo turbine is limited and indicates that current theory and experimental knowledge do not adequately explain the effects of certain design parameters, such as nozzle diameter, jet inlet angle, number of blades, and blade speed on the turbine's efficiency. In this study, these parameters are used in a three-level (3^4) central composite response surface experiment. A low-cost Turgo turbine is built and tested from readily available materials and a second order regression model is developed to predict its efficiency as a function of each parameter above and their interactions. The effects of blade orientation angle and jet impact location on efficiency are also investigated and experimentally found to be of relatively little significance to the turbine. The purpose of this study is to establish empirical design guidelines that enable small hydroelectric manufacturers and individuals to design low-cost efficient Turgo Turbines that can be optimized to a specific pico-hydro site. The results are also expressed in dimensionless parameters to allow for potential scaling to larger systems and manufacturers.

1. Introduction

The Turgo turbine is a hydroelectric impulse turbine that has gained renewed attention in research because of its potential application to millions of off-grid 5 kW-or-less pico-hydro sites and to energy recovery of discharged water at public water systems [1]. Generally, pico hydro systems are run of the river, which means that impoundment is not necessary. Such a scheme diverts water from the river as needed, feeding it down a steep slope through a penstock, a nozzle and then the turbine, after which the effluent water rejoins the river or is used for irrigation and other community purposes.

In developing countries alone, where 1.6 billion people live without electricity, a recent study showed that there are 4 million potential pico-hydro sites [2]. Furthermore, a World Bank study in 2006 showed that pico-hydropower is the most competitive off-grid power technology on a levelized cost of electricity (LCOE) basis ($/kWh), as shown in Fig. 1 [3,4]. In Rwanda for example, the national utility retail price for electricity in 2009 was $0.24/kWh [5], yet pico-hydro is estimated to cost less than $0.20/kWh. Nevertheless, the installation cost ($/kW) of pico-hydro systems can become cost prohibitive. In 2011, Meier reported a study of 80 Indonesian villages that revealed capital costs per kW exponentially increase with smaller sized systems, potentially surpassing $10,000/kW for low-head systems less than 5 kW [6]. Within the United States it is currently understood that sites with less than 100 kW of electrical potential are “best left undeveloped” because of extremely high installation costs ($59,000/kW on average) [7].

To reduce capital costs, standardized off-the-shelf turbines, as opposed to turbines that are customized to a specific site, are sold commercially by manufacturers worldwide, including the United States, Canada, and China [8–13]. The cost of these pico-hydro turbines can range from $125/kW to over $1200/kW. The

* Corresponding author.
E-mail addresses: kbgaiser@ucdavis.edu (K. Gaiser), paerickson@ucdavis.edu (P. Erickson).

http://dx.doi.org/10.1016/j.renene.2015.06.049
0960-1481/

Nomenclature

α	jet inlet angle
β	relative jet angle with respect to the blade
b	parameter coefficient of linear regression equation
C_p	Mallow's statistic
c_D	discharge coefficient of nozzle
c_v	velocity coefficient of nozzle
δ	angle of blade curvature
D	pitch to center diameter of the turbine (PCD)
d	nozzle diameter
g	acceleration of gravity
H	hydraulic head
k	friction coefficient factor
η	efficiency
$\widehat{\eta}$	predicted value from regression equation
N_{sp}	specific speed (units of rev/s or rpm)
Ω_{sp}	specific speed (units of radians)
φ	speed ratio
P	power
p	pressure
Q	flow of water
ρ	density of water
R	relative velocity of jet with respect to blade
R^2_{adj}	adjusted R^2 statistic
s	spacing between blades
τ	torque
θ	angle of the blade's edge: inlet (θ_1) or exit (θ_2).
μ	viscosity of water
u	blade velocity
v	jet velocity
w	width of the blade
ω	turbine angular velocity
X	coded variable, between −1 and 1
Z	number of blades

Acronyms

ANOVA	Analysis of Variance
BEP	best efficiency point
CCD	central composite design
LCOE	levelized cost of energy
MSE	mean square error
MSPR	mean square predicted residual
PCD	Pitch to Center Diameter (D)
PRESS	Predicted Sum of Squares
SAS	statistical analysis software
VIF	Variance Inflation Factor

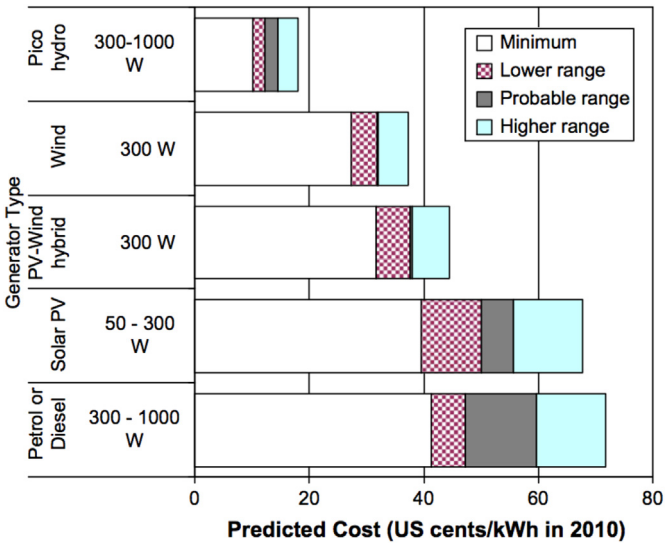

Fig. 1. Cost of pico-hydro systems compared to common alternatives (used with permission from Elsevier) [3].

mechanical efficiency in a laboratory testing environment can be upward of 82%, which is typical of a well-manufactured Turgo machine [14]. However, because standardized turbines are not customized to a specific site, they are prone to be less efficient in the field, some reporting only 40% water-to-wire efficiency [8]. Furthermore, off-the-shelf systems shipped abroad are more difficult and costly to repair and maintain in-country due to the system's proprietary design, the dependency upon imported spare parts with lengthier lead times, which results in longer power outages, and taxes levied by customs, which have been shown to increase equipment costs by 40% on pico-hydro systems [2].

Simpler do-it-yourself turbines reduce installation costs, but these turbines usually suffer from poor efficiencies due to a lack of design guidelines, fabrication facilities, or technical expertise. An example of a simple turbine built in Rwanda is shown in Fig. 2. Meier's assessment of pico-hydropower in Rwanda estimated that simple improvements in turbine design could increase efficiency by 20% with no additional equipment cost [6].

Therefore, this study aims not to build a standardized off-the-shelf turbine, but to develop a set of standardized design equations for optimizing the most important parameters of a Turgo turbine based on a site's available head and flow. This approach can facilitate the custom design and local manufacture of low-cost, yet efficient Turgo turbines. In the present study, a Turgo turbine is built from materials of low cost and a set of empirical design equations is established for optimizing the Turgo turbine's most significant parameters. Specifically, the nozzle diameter, d, jet inlet

Fig. 2. A locally fabricated impulse turbine in Rwanda (Photograph by Kyle Gaiser).

angle, α, number of blades, Z, dimensionless blade speed, φ, jet impact location, and blade orientation angle, are investigated to determine if and how they influence the turbine's efficiency, η.

2. Pico-hydropower background

The suitability of a hydroelectric turbine to a particular site depends on the site's head, H, and water flow rate, Q. Impulse turbines, such as the Pelton and Turgo, are suited for sites with high head and low flow, while reaction turbines operate best at low head and high flow conditions. The difference between the Pelton and Turgo turbines is illustrated in Fig. 3 [15]. Water strikes the bucket of a Pelton wheel in the same plane as the wheel, then splits in half, reverses, and discharges at both sides. The jet of a Turgo turbine is angled to one side of the turbine's plane and the discharged water exits out the other side after being reversed by the blades.

The available hydraulic power, P_H, of a hydraulic turbine is a function of the head and flow:

$$P_H = \rho g H Q \tag{1}$$

Meanwhile, the turbine's mechanical power output, P_M, is the product of the torque, τ, and rotational velocity, ω:

$$P_M = \tau\omega \tag{2}$$

A turbine's experimental efficiency is:

$$\eta = \frac{P_M}{P_H} \tag{3}$$

As a momentum transfer machine, the Turgo turbine's theoretical efficiency can be calculated by the change in the water's velocity between the inlet and outlet of the blade. Fig. 4 depicts the velocity vectors as a jet of water impacts a single Turgo blade [16]. The reference direction is that of the blade velocity, u. The water enters with an absolute velocity, v_1, an angle, α_1, a relative velocity, R_1, with respect to the blade's reference frame, and a relative angle β_1. The relative inlet angle of the water is assumed to be parallel to the blade's inlet edge for smooth entry in order to prevent hydraulic shock, or water hammer [17]. When the nozzle and blade are oriented this way the condition is known as the "no-shock" condition, $\alpha_{no-shock}$.

The absolute inlet velocity can be calculated by:

$$v_1 = c_v\sqrt{2gH} \tag{4}$$

where c_v is a constant called the coefficient of velocity. The relative inlet angle can be expressed as:

$$\beta_1 = \tan^{-1}\left(\frac{\sin\alpha_1}{\cos\alpha_1 - \varphi}\right) \tag{5}$$

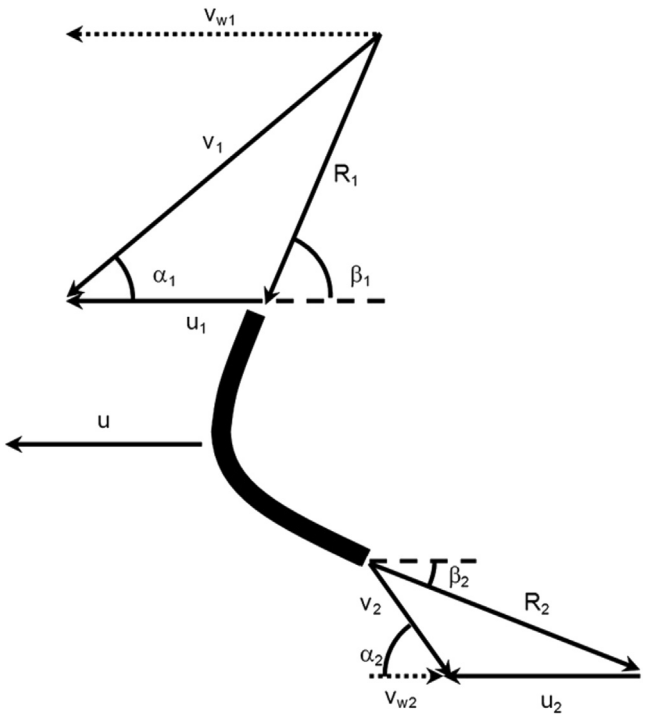

Fig. 4. Velocity vector triangle diagram of a single Turgo blade (Adapted from Williamson [32]. Used with permission from Elsevier).

where φ is the speed ratio, defined as:

$$\varphi \equiv u/v_1 = \cos\alpha_1 - \frac{\sin\alpha_1}{\tan\beta_1} \tag{6}$$

The Turgo blade causes the fluid to change direction and exit at a relative angle β_2, which is equal to the blade's discharge angle. The relative effluent velocity is R_2 and its absolute velocity is v_2.

Using the velocity triangles, the theoretical hydraulic efficiency can be expressed as [18]:

$$\eta_H = 2c_v^2\left(\varphi\cos\alpha_1 - \varphi^2 + \frac{k\varphi\sin\alpha_1\cos\beta_2}{\sin\beta_1}\right) \tag{7}$$

where the constant k is a friction coefficient equal to the ratio of relative exit velocity to relative inlet velocity (R_2/R_1). k is typically 0.90–0.95 for a well-designed blade [17].

Using Equation (7), efficiency is plotted as a function of speed ratio in Fig. 5, for jet inlet angles ranging from 10° to 40°, $c_v = 1$ and $\beta_2 = 15°$. For every value of α, there exists an optimum speed ratio, φ_{opt}, called the Best Efficiency Point (BEP) of the turbine, and a corresponding relative jet inlet angle, $\beta_{1,opt}$, which is theoretically

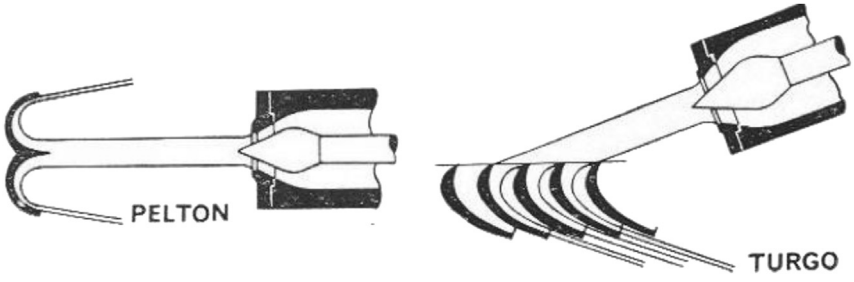

Fig. 3. Difference in direction of water flow between the Pelton (left) and Turgo (right) Turbines [15].

equal to the blade's inlet angle in order to satisfy the no-shock condition. The converse is true as well: for fixed inlet and exit blade angles there exists a theoretical φ_{opt} and $\alpha_{no\text{-}shock}$, which is theoretically equal to α_{opt}. These can be calculated when the derivatives of Equations (7) and (6) are substituted and solved for each other. Upon inspecting Fig. 5, an approximation of $\alpha_{no\text{-}shock}$ for small angles, which Gibson explains in detail [17], is simply,

$$\alpha_{no-shock} = \frac{\beta_1}{2} \tag{8}$$

In the special case of a Pelton wheel, $\alpha_1 = 0$, and the BEP is at $\varphi_{opt} = 0.5$. However, because Turgo turbines have a non-zero inlet angle, the theoretical BEP depends upon α_1 and β_2. Note that the β_1 term from Equation (7) can be expressed in terms of α_1 and φ by rearranging and substituting Equation (6).

3. Previous work

Unlike the Pelton, relatively little experimental research for the Turgo has been documented [16]. The Turgo turbine is usually treated the same as the Pelton Wheel, despite their differences [19,20]. While the Pelton has a slightly higher theoretical efficiency, the Turgo has several distinct advantages. The Turgo Turbine's Pitch to Center Diameter (PCD) can be half the diameter of the Pelton, resulting in less wind resistance and higher RPMs, which is better for generator matching [15,21,22]. The Turgo is also known for its flat efficiency curve, meaning its performance is less sensitive to changes in flow rate, which is most pertinent to run-of-the-river pico-hydro systems [14,23].

Several key experimental findings regarding the Turgo turbine and the literature's limitations are described below.

3.1. Jet inlet angle

While theory states that the optimum angle of attack is $\alpha_{no\text{-}shock}$, in practice, α_{opt} is usually a *few degrees less* than $\alpha_{no\text{-}shock}$ [18]. However, if the difference is too large then hydraulic shock can occur and energy is lost due to eddies circulating counter to the flow.

Furthermore, a theoretical expression for α_{opt} can be formulated by taking the derivative of Equation (7) with respect to α. By substituting Equation (6), β_1 drops out and α_{opt} becomes a function of speed ratio and relative exit angle only. However, several recent studies have suggested that α_{opt} depends on other factors such as the number of blades and the nozzle diameter, but these interactions have yet to be quantitatively characterized. A 2013 study on pico-hydro Turgo turbines by Williamson [16] revealed that the optimum inlet angle depends on the nozzle diameter. For example, for a 20 mm nozzle, $\alpha_{opt} = 10°$ but for a 30 mm nozzle, $\alpha_{opt} = 20°$, which suggests that a larger nozzle diameter requires a larger jet angle. In 2012, Cobb [20] reported α_{opt} to be 18–20° for a Turgo of 28 blades and comparable PCD to Williamson's, which used only 9 blades. Furthermore, in 2011, Koukouvinis et al. [24] reported an optimum jet inlet angle of 30°, with a 7–10 point drop in efficiency at angles ± 10°. Other published sources have assumed $\alpha_{opt} = 25°$ [21], 20° [23], and 30° [25] but without an explanation as to what factors lead to such different values.

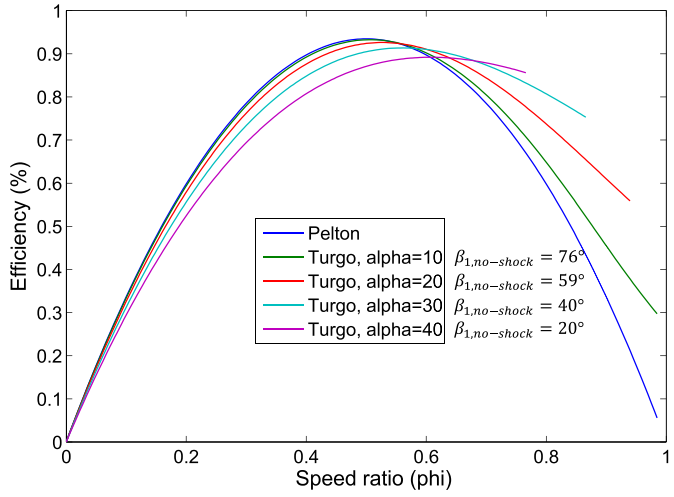

Fig. 5. Efficiency curves of a Pelton and an impulse turbine of changing jet inlet angle.

3.2. Blade exit angle and best efficiency point

According to Equation (7), the relative exit angle, β_2, should be as small as possible; however, if the angle is too small the effluent water will interfere with the oncoming blade. Experiments indicate that a discharge angle of 15–20° performs the best [17,26,27]. Furthermore, as stated previously, according to theory, φ_{opt} is a function of α_1 and β_2 only. However, it is known that the actual BEP is usually less than the theoretically predicted φ_{opt} [16]. Therefore, Equation (7) does not adequately explain the factors that contribute to $\beta_{2,opt}$ and φ_{opt}.

3.3. Effect of nozzle diameter

The blade width to nozzle diameter ratio (w/d) has an important influence on the way water flows over a curved surface [28]. As this ratio decreases there is increasing turbulence and re-circulation, which disrupts the flow. For a Pelton, the w/d ratio is usually between three and five [17,18,29]. A study in 2007 suggested $w/d = 1.45$ for the Turgo, but without justification [21].

In his review of the Turgo turbine's history, Wilson stated that another dimensionless ratio, D/d, decides all the main characteristics of an impulse turbine [15]. While a smaller D/d is desirable for faster speeds, if it becomes too small it could result in flow limitations [30]. Several sources report that the ratio of D/d for a Pelton wheel should be no less than 10:1 [15,17,18,27,29]. The Turgo turbine is capable of cutting this ratio in half, at least [15,17,24,31].

In a recent Turgo turbine study, Williamson [16] tested five nozzle diameters: 10, 15, 20, 25, and 30 mm. The associated turbine efficiencies are plotted in Fig. 6. The best performing design was $d = 20$ mm, which corresponds to 1.75 w/d and 7.5 D/d. The efficiency dropped drastically for larger nozzles, by up to 30% with the

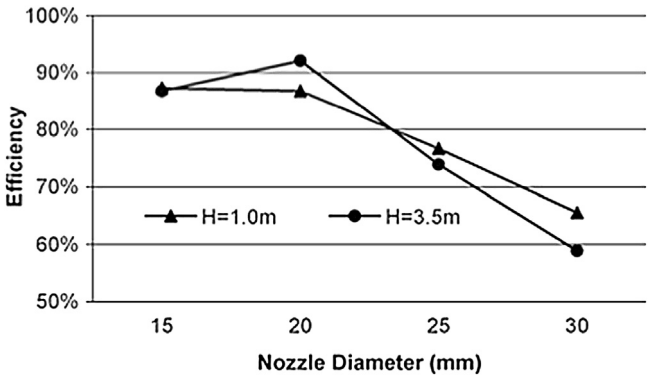

Fig. 6. Effect of nozzle diameter on efficiency (used with permission from Elsevier) [16].

30 mm nozzle ($w/d = 0.86$ and $D/d = 5$). In Cobb's 2013 study the nozzle diameter did not significantly affect the efficiency, but the D/d ratio remained greater than 10 and the ratio w/d was always 2.25 or greater, both of which are large values.

3.4. Effect of multiple blades

The velocity triangle calculations only apply to a single Turgo blade and do not capture the effect of multiple blades. The optimum number of blades for a Pelton turbine is given by Tygun's empirical formula [25,32]:

$$Z = 15 + \frac{D}{2d} \tag{9}$$

In addition to citing Tygun's formula, Kadambi [29] and Thake [27] have published a chart for determining the best number of blades on a Pelton wheel based on the ratio D/d.

While these design equations exist for the Pelton, no empirical formula or suggested optimum number of blades exists for the Turgo turbine, to the authors' knowledge. The number of blades reported in literature varies drastically without explanation. Williamson's turbine used 9 blades [16], while Cobb's used 28 blades [14] for similar PCDs. Furthermore, a sketch in Harvey's *Micro-Hydro Design Manual* [23] depicts that the jet should be split between three blades simultaneously, suggesting that the ratio of nozzle diameter to blade spacing ratio (d/s) is important. Gulliver and Singh [33,34] recognize that additional blades could be beneficial because it would allow the turbine to handle higher flows, which is akin to adding multiple nozzles. Nevertheless, the optimum number of blades and the interactions amongst blade number, jet angle and nozzle diameter has not been thoroughly investigated for the Turgo turbine.

3.5. Jet's axial impact location

Williamson also investigated the effect of the jet's axial impact location on Turgo efficiency [16]. "Axial" refers to the location along the width of the blade from entry to exit. The results, shown in Fig. 7, indicate that the best efficiency occurred at an impact location 6 mm inside the entry edge of the blade, which corresponds to roughly one-sixth the width of the blade. Misaligning the jet by 4–6 mm (11%–17% of the width) resulted in a 10% drop in efficiency.

3.6. Turbine power specific speed

The non-dimensional power specific speed, Ω_{sp}, is a parameter that assists engineers in selecting the best type of turbine for a site, independent of the turbine's size [18]. For example, if the specific speed is between 0.094 and 0.15, then a single jet Pelton wheel is appropriate, whereas a low head Francis turbine would be suited to specific speeds between 0.34 and 2.3. The power specific speed is given by:

$$\Omega_{sp} = \left(\frac{\omega P_M^{1/2}}{\rho^{1/2} (gH)^{5/4}} \right)_{\eta = \eta_{max}} \tag{10}$$

and is evaluated at the maximum efficiency point. This is equivalent to the less common form [30]:

$$\Omega_{sp} = \left(2\sqrt{2}\, \pi\, \eta_{max} \right)^{1/2} \varphi \frac{d}{D} \tag{11}$$

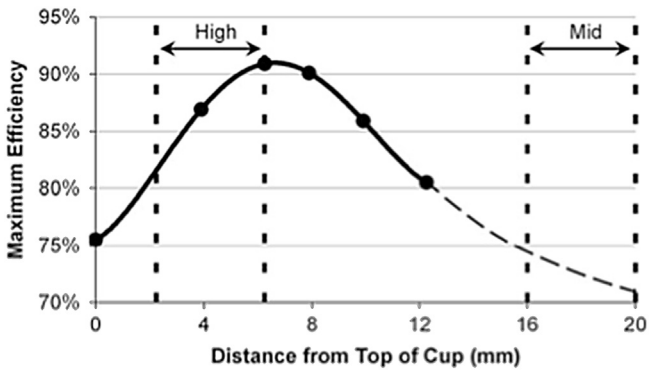

Fig. 7. Effect of jet axial impact location on maximum efficiency (used with permission from Elsevier) [16].

3.7. Contribution to the literature

First, this study sets out to quantitatively determine the effect of blade number, jet angle, nozzle diameter, and speed ratio on a low-cost Turgo turbine's efficiency. By means of regression analysis, a prediction equation will provide a more complete picture of how these factors affect efficiency and how they interact with one another. The prediction equation will also enable each parameter to be optimized for a site's flow characteristics. Dimensionless parameters, such as d/s, w/d and the specific speed will be considered to help establish design guidelines for the Turgo. Furthermore, this study will probe the sensitivity of the UC Davis Turgo turbine's efficiency to variations in the jet's axial impact location and the blades' orientation angle (inlet and outlet angles).

Table 1 compares the design parameters of the UC Davis Turgo turbine to that of pico-hydro Turgo turbines used in recent literature by Cobb [20] and Williamson [16].

4. Methodology

A low-cost Turgo turbine, shown in Fig. 8, was built at UC Davis. The cost of the turbine's materials was approximately $30. Tablespoons were chosen for blades because they are common, inexpensive, made of stainless steel for rust and pitting resistance, and have dimensional similarity to other Turgo blades, such as those used by Cobb and Williamson. The spoon's angle of curvature was measured to be $\delta = 82°$, as shown in Fig. 9. The blade was rotated 30° from the hub's face, resulting in a blade inlet angle of $\theta_1 = 79°$ and exit angle of $\theta_2 = 19°$, which is assumed to be equal to β_2. With these inlet and exit angles and a friction factor of $k = 0.9$, the theoretical hydraulic efficiency of the turbine (Equation (7)) is approximately $\eta_H = 90\%$, and using Equations (6) and (7), $\alpha_{no\text{-}shock} = 42°$, and. $\varphi_{opt} = 0.62$.

An adjustable nozzle mount allowed for adjustments to the nozzle angle, height and distance away from the turbine (Fig. 10). Water was supplied from the 150-foot tall domestic water tower at UC Davis. An analog pressure gauge was placed directly before the nozzle and the dynamic pressure was held constant at 50 ± 0.5 psi for every test because turbine efficiency and BEP have been shown to be independent of the water pressure [20], Three nozzles were used and the coefficient of discharge, c_D, was taken to be 0.95 for all tests [35]. The nozzle dimensions and test conditions are shown in Table 2.

An 18 cm water-brake dynamometer from Land & Sea, Inc. was used for turbine load control and measurement of the turbine's torque and rpm. The turbine produced power ranging upward of 1.4 kW (1.9 Hp) at 1650 rpm down to 0.06 kW (0.082 Hp) at

Table 1
Comparison of the proposed turbine's design parameters to those previously researched.

Turbine design parameter	UC Davis (Gaiser et al.)	Cobb et al. [20] (169 mm)	Cobb et al. [20] (131 mm)	Williamson et al. [16]
Turbine PCD, D (mm)	130	169	131	150
Number of blades, Z	10–20	28	20	9
Blade spacing, s (mm)	40.8, 27.2, 20.4	19.0	20.6	52.4
Nozzle diameter, d (mm)	7.125, 12.85, 18.59	7.94–12.70	7.94–12.70	15–30
Jet angle, α (degrees)	10–40	14–24	14–24	10–40
Width, w (mm)	39	28.6	28.6	35
Height (mm)	61	38.09	38.09	–
Thickness (mm)	1.06	2.38	2.38	–
Volume, V (mL)	15	7.932	7.932	–
Curvature radius (mm)	30	15.75	15.75	–
Inlet angle, theta1 (deg)	79	45	45	–
Discharge angle, theta2 (deg)	19	–	–	–
Head (m)	35	18–28	17–25	0.5–3.5
Dimensionless ratios				
D/d	6.99–18.25	15.2–21.3	10.3–16.5	10–5
Ω_{sp}	0.027–0.142	0.057–0.081	0.072–0.117	–
d/s	0.17–0.91	0.42–0.67	0.39–0.62	0.38–0.57
w/d	5.3–2.04	2.25–3.6	2.25–3.6	2.3–0.86

Fig. 8. Twenty-blade tablespoon turbine built at UC Davis.

360 rpm, for various turbine and nozzle configurations.

4.1. Dimensional analysis

Dimensional analysis can be used to express the functional relationship between the efficiency of a hydroelectric turbine and its independent design variables [36,37]. Fourteen independent design parameters were identified:

$$\eta = f[\alpha, Z, d, D, \omega, \theta_1, \theta_2, \nu, w, V, \rho, g, \mu\,] \tag{12}$$

In this case, the number of blades, Z, is used rather than the spacing between blades, s, although they are related by the turbine's circumference, πD. V is the blade's volume and μ, the viscosity of water. A non-dimensional relationship with fewer dimensionless independent parameters can be obtained according to the Buckingham Pi theorem. Using D, ν, and ρ as control variables, the dimensionless Equation (13) was developed by application of the Ipsen method, as outlined by Gray [38].

$$\eta = f\left(\alpha, Z, \frac{d}{D}, \frac{\omega D}{\nu}, \theta_1, \theta_2, \frac{V}{D^3}, \frac{w}{D}, \frac{\mu}{\rho \nu D}, \frac{gD}{\nu^2}\right) \tag{13}$$

On the left side of the equation, η, efficiency, is the response variable. On the right side, $\omega D/\nu$ is the speed ratio, $\mu/\rho\nu D$ is the Reynolds number, and gD/ν^2, the Froude number. By Equation (11) the product of terms three and four, $\frac{d}{D} \times \frac{\omega D}{\nu}$, is directly proportional to the specific speed of the turbine, and the product of $Z \times \frac{d}{D}$ is proportional to the ratio d/s.

To decrease the number of variables for testing, the spoon volume, V, turbine diameter, D, and water pressure, represented by velocity, ν, were held constant. Turbine performance is typically insensitive to the Reynolds number, which makes this parameter of little interest [18]. Similarly, the Froude number is not explored. Finally, α is replaced with $\sin(\alpha)$ to account for the trigonometric nature of the velocity vector triangles. This results in a function with four independent factors:

$$\eta = f\left(\sin\alpha, Z, \frac{d}{D}, \frac{\omega D}{\nu}\right) \tag{14}$$

4.2. Experiment design and procedure

A response surface method is a common statistical technique used to empirically model the relationship between a response variable (output, such as efficiency) and several independent parameters (input variables), with the objective of optimizing the response. Through a carefully constructed design of experiment, such as a central composite design (CCD), the cost of optimization can be reduced when compared to more complex methods such as CFD analysis. A three-level face-centered CCD [37,39] is used to develop a complete second order four-factor regression equation:

$$\begin{aligned}\widehat{\eta_i} = {} & b_0 + b_1X_{i1} + b_2X_{i2} + b_3X_{i3} + b_4X_{i4} + b_{11}X_{i1}^2 + b_{22}X_{i2}^2 \\ & + b_3X_{i3}^2 + b_4X_{i4}^2 + b_{12}X_{i1}X_{i2} + b_{13}X_{i1}X_{i3} + b_{14}X_{i1}X_{i4} \\ & + b_{23}X_{i2}X_{i3} + b_{24}X_{i2}X_{i4} + b_{34}X_{i3}X_{i4}\end{aligned} \tag{15}$$

In Equations (15), X1 is jet angle, X2 is number of blades, X3 is nozzle diameter, X4 is speed ratio, "i" indicates the replicate number, and the b-terms are the coefficients to be determined by

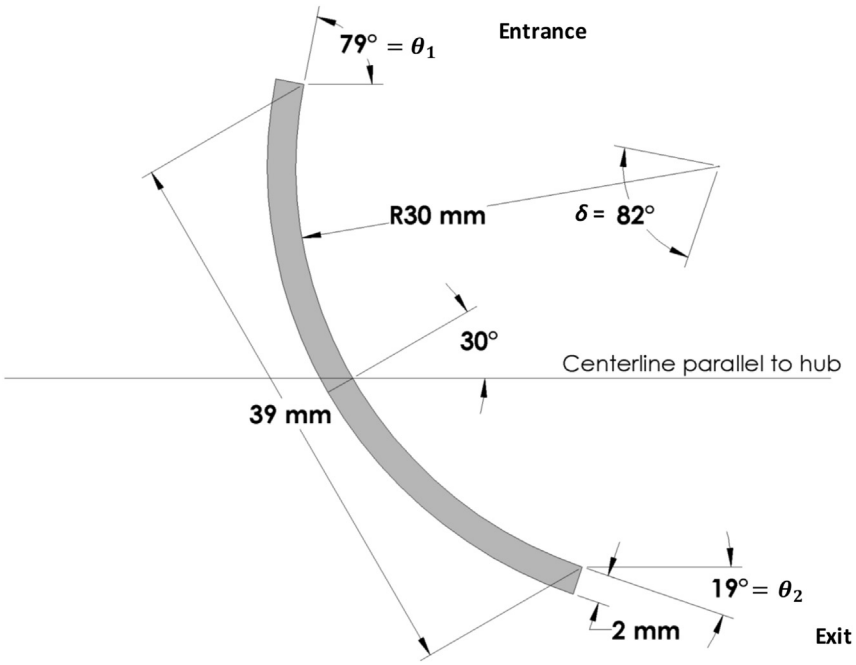

Fig. 9. Dimensions and orientation of the tablespoon blade.

experimentation. The null hypotheses for each term in Equation (15) state that the parameter's *b*-term is zero, which would relegate the parameter insignificant. A confidence level of 95% is used to guard against the incorrect rejection of a true null hypothesis. SAS software is used to conduct a series of t-tests on each parameter and to check for multicollinearity within the data. Stepwise selection methods were employed and the C_p, R^2_{adj}, and Predicted Sum of Squares (*PRESS*) values, all of which assess the fit of a regression line, were used to select the best model.

To reduce multicollinearity, the three levels are evenly spaced and converted to coded units: +1, −1 and 0, such that, for example, X1 is a function of α. The levels for each factor are summarized in Table 3 and are chosen so that a wide range of values relevant to previous literature is tested (see Table 1).

Five additional replicates are performed at each of the points (0, 0, 0, 0), (0, 0, 0, −1), and (0, 0, 0, 1), in order to have a good estimate of the pure error [40]. The total number of data points was $3^4 + 15 = 96$; however, the factor X4, speed ratio (i.e. RPM), was decreased continuously during each experiment, so in effect 31 randomized experiments were performed. As the RPM decreased, the torque was recorded and Equations (1)–(3) were used to calculate efficiency and Equation (16) to calculate speed ratio.

$$\varphi = \frac{u}{v} = \frac{\pi D(RPM)}{60\sqrt{2gH}} \tag{16}$$

Fig. 11 is an example where X1, X2, and X3 are zero. A best-fit

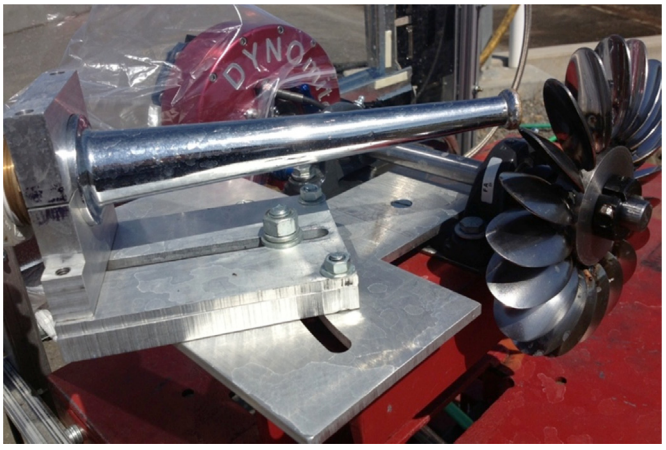

Fig. 10. The UC Davis Turgo Turbine and adjustable nozzle apparatus.

Table 3
Factors and factor levels tested.

Level	Coded variable	−1	0	1
Jet angle, α (degrees)	X1	10	25	40
Number of blades, *Z*	X2	10	15	20
Nozzle diameter, d (mm)	X3	7.13	12.85	18.60
Speed ratio, φ	X4	0.25	0.35	0.45
sinα, X1	X1	0.174	0.423	0.643
Z, X2	X2	10	15	20
d/*D*, X3	X3	0.055	0.099	0.143
Speed ratio, φ, X4	X4	0.25	0.35	0.45

Table 2
Nozzle diameters and operating flow rates.

Name	Diameter (±0.013 mm)	Diameter (±0.0005 in)	Measured flow rate @ 50 psi (L/s)	Hydraulic power (kW)
¾″ nozzle	18.593	0.7320	7.13 (113.0 GPM)	2.455
½″ nozzle	12.852	0.5060	3.42 (54.2 GPM)	1.185
¼″ nozzle	7.125	0.2805	1.05 (16.7 GPM)	0.366

2nd order polynomial is fitted to the data and the efficiencies at the three predetermined levels of speed ratio ($\varphi = 0.25$, 0.35 and 0.45), shown by the vertical dotted lines, are extracted.

5. Results and discussion

5.1. Multiple linear regression analysis

Of the 96 trials, three data points had standard deviations greater than 2.5 from the predicted value. These points were taken with a faulty pressure gauge, which was replaced in subsequent tests. The outliers were removed and the Mean Standard Error (*MSE*) noticeably improved.

The four independent variables, blade angle (X1), number of blades (X2), nozzle diameter (X3) and speed ratio (X4) were used in SAS to determine the coefficients in the regression Equation (15). The removal of X1 results in the best regression fit in which all the parameters are significant at a 95% confidence level, as indicated by the p-values in the in the "Pr > |t|" column of Table 4. The Variance Inflation Factors were all less than 10, indicating no multicollinearity. The ANOVA table indicates that the overall model is also significant. The R^2_{adj} is high (0.938) and the RMSE is a minimum at ± 2.20.

From the parameter estimates in Table 4, the prediction equation is written in its coded form:

$$\begin{aligned}\hat{\eta} = {} & 57.68 + 3.64X_2 + 5.66X_3 + 1.43X_4 - 4.17X_1^2 - 2.04X_2^2 \\ & - 8.15X_3^2 - 4.94X_4^2 + 3.42X_1X_2 + 0.98X_1X_3 - 1.56X_1X_4 \\ & - 0.75X_2X_3 + 2.95X_2X_4 + 2.98X_3X_4\end{aligned} \tag{17}$$

All four factors have a significant second-order effect on the efficiency of the turbine, with the nozzle diameter (X3) having the largest effect. All of the interaction terms are significant too. It is more useful to express X1, X2, X3 and X4 in terms of dimensionless parameters, sin(α), *Z*, *d/D* and φ, respectively. Substituting results in Equation (18), which is valid within the domains outlined in Table 3.

$$\begin{aligned}\hat{\eta} = {} & -42.077 + 32.772\sin\alpha + 0.243Z + 732.42\frac{d}{D} + 232.25\varphi \\ & - 75.786\sin^2\alpha - 0.0816Z^2 - 4191.2\left(\frac{d}{D}\right)^2 - 494\varphi^2 \\ & + 2.916Z\sin\alpha + 94.770\frac{d}{D}\sin\alpha - 66.505\varphi\sin\alpha \\ & - 3.4060\frac{d}{D}Z + 5.9\varphi Z + 675.61\frac{d}{D}\varphi\end{aligned} \tag{18}$$

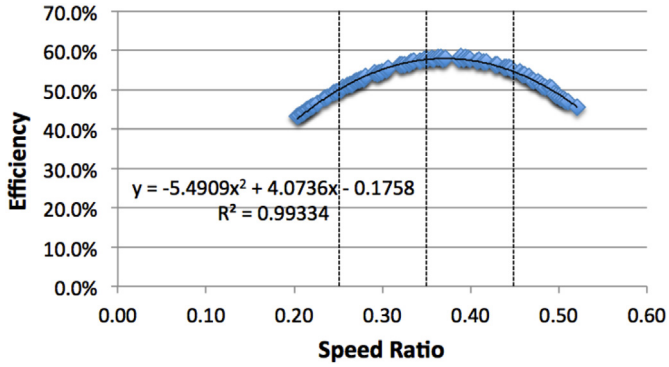

Fig. 11. Test result for (0,0,0,x), with a best-fit curve.

Table 4
ANOVA and parameter estimates for the best regression model.

Analysis of variance					
Source	DF	Sum of squares	Mean square	F Value	Pr > F
Model	13	6807.78	523.68	108.56	<0.0001
Error	79	381.08	4.8238		
Corrected total	92	7188.86			

Root MSE	2.1963	R-Square	0.9470
Dependent mean	46.045	Adj R-Sq	0.9383
Coeff var	4.7700		

Parameter estimates								
Variable	DF	Parameter estimate	Standard error	t value	Pr > |t|	Variance inflation	95% confidence limits	
Intercept	1	57.684	0.55546	103.85	<0.0001	0	56.579	58.790
X2	1	3.6406	0.29888	12.18	<0.0001	1.0000	3.0457	4.2355
X3	1	5.6597	0.29888	18.94	<0.0001	1.0000	5.0648	6.2546
X4	1	1.4312	0.27894	5.13	<0.0001	1.0001	0.8760	1.9864
X12	1	−4.1687	0.47812	−8.72	<0.0001	1.0748	−5.1204	−3.2171
X22	1	−2.0428	0.47852	−4.27	<0.0001	1.0749	−2.9953	−1.0903
X32	1	−8.1534	0.47852	−17.04	<0.0001	1.0749	−9.1058	−7.2009
X42	1	−4.9409	0.48312	−10.23	<0.0001	1.0000	−5.9026	−3.9793
X1X2	1	3.4193	0.36582	9.35	<0.0001	1.0000	2.6911	4.1474
X1X3	1	0.9802	0.36582	2.68	0.0090	1.0000	0.2520	1.7084
X1X4	1	−1.5552	0.36576	−4.25	<0.0001	1.0001	−2.2832	−0.8271
X2X3	1	−0.7463	0.36605	−2.04	0.0448	1.0000	−1.4749	−0.0177
X2X4	1	2.9535	0.36605	8.07	<0.0001	1.0000	2.2249	3.6821
X3X4	1	2.9760	0.36605	8.13	<0.0001	1.0000	2.2474	3.7047

5.2. Residual analysis

Linear regression assumes that the error terms are normally distributed, independent and identically distributed. Fig. 12 shows residual analysis plots for the data. A histogram of the residuals and a normal QQ plot both confirm the normality of the error terms and a plot of the R-studentized residuals versus predicted value confirms that the residuals are identically distributed with no significant outliers. The chronological plot indicates the residuals are sufficiently random with respect to time.

5.3. Model validation

To validate the model, fourteen new experiments were conducted at various levels of each factor, including new angles of 15 and 30°. The value of φ that corresponded to the experimental BEP was used. To measure the predictive ability of the selected model, the mean squared prediction error is calculated, as defined by Kutner [40]. The validation cases are shown in Table 5.

Because the *MSPR* (4.28) is less than the *MSE* (4.82), located in the ANOVA table (Table 4) the *MSE* is retained as an accurate indication of the model's predictive ability.

5.4. Optimization and comparison to literature

Due to the second-order nature of the prediction equation, the predicted optimum value of each factor can be obtained. The partial derivative of Equation (18) is taken, set equal to zero and solved with respect to the factor under consideration. This results in four unique design equations, which are used to express the optimum value of each factor in terms of the other three factors.

$$\alpha_{opt} = \sin^{-1}\left(0.0192Z + 0.624\frac{d}{D} - 0.4388\phi + 0.2162\right) \tag{19}$$

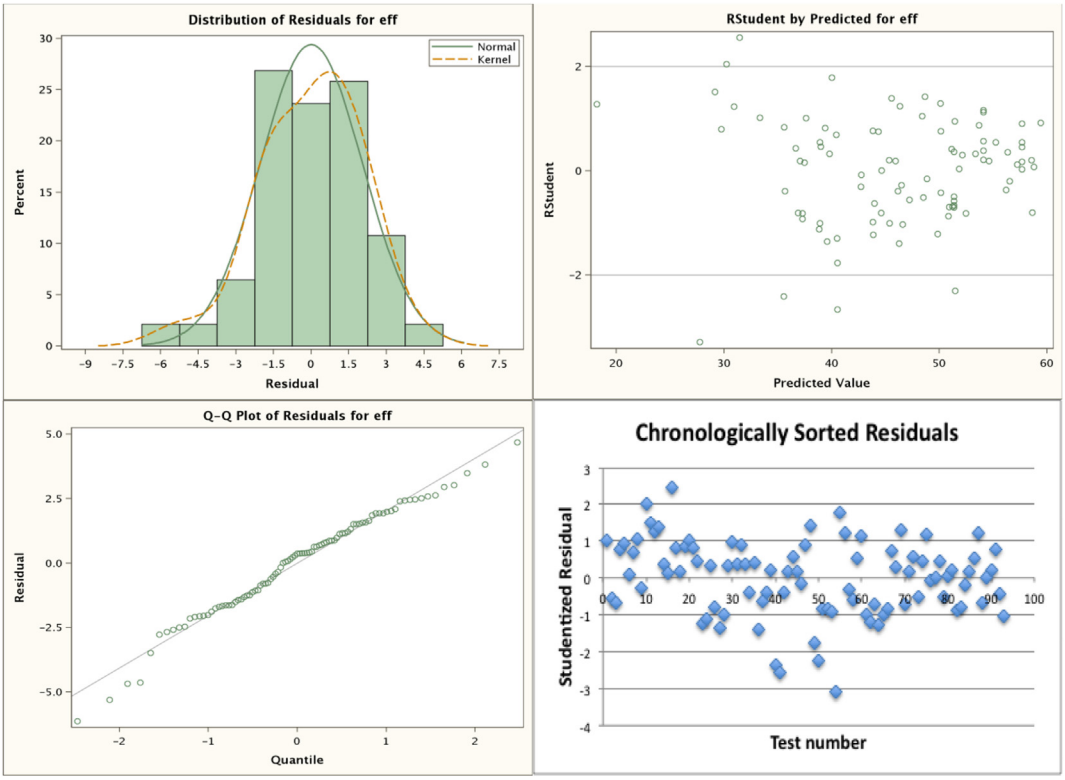

Fig. 12. Residual analysis plots for the 4-factor CCD experiment.

Table 5
Validation experiments for the best-selected model.

Trial i	Angle α	Blades Z	Diameter d	Speed ratio φ	Predicted $\widehat{\eta_i}$	Observed η_i
1	15	20	7.125	0.337	42.4	43.7
2	25	20	7.125	0.322	45.6	42.5
3	30	20	7.125	0.307	45.3	42.8
4	10	15	18.593	0.430	51.5	51.0
5	20	15	18.593	0.412	55.6	54.7
6	20	20	18.593	0.447	57.3	55.3
7	30	20	18.593	0.409	59.4	60.4
8	10	20	18.593	0.430	51.2	52.9
9	30	20	12.852	0.391	60.7	61.0
10	30	20	12.852	0.399	60.6	62.5
11	30	20	12.852	0.392	60.7	62.4
12	30	20	12.852	0.403	60.6	64.7
13	30	20	12.852	0.389	60.7	61.9
14	30	20	12.852	0.393	60.7	63.8
MSPR						**4.28**
Root MSPR (sigma)						±2.07

$$Z_{opt} = 17.87 \sin\alpha - 20.8\frac{d}{D} + 36.15\phi + 1.49 \quad (20)$$

$$d_{opt} = 0.0113 \sin\alpha - 0.0004Z + 0.0806\phi + 0.0874 \quad (21)$$

$$\varphi_{opt} = -0.0673 \sin\alpha + 0.0060Z + 0.689\frac{d}{D} + 0.2351 \quad (22)$$

By substitution, this system of equations is solved to find the optimum values for the turbine:

$$\alpha_{opt} = 35.4^{\circ}$$
$$Z_{opt} = 25\ blades$$
$$d_{opt} = 15.4\ mm (d/D = 0.118)$$
$$\varphi_{opt} = 0.425$$

The predicted efficiency of the turbine under these conditions is $\eta_{opt} = 63\%$, lower than the theoretical efficiency of 89%. This discrepancy is likely due to the relatively large skin friction and eddy formation inherent to using low cost tablespoons [17]. The optimum value of D/d is 8.5, which is consistent with literature. Note that the optimum blade number of 25 is outside of the experimental domain and because it is extrapolated it cannot be

completely trusted. However, Z_{opt} can be, and often is, within the tested domain (10–20), depending on the values of the other parameters.

Fig. 13 is a photograph depicting the physical flow of the water through the turbine at low speed. The water enters from the right, splits between two blades, reverses direction and exits to the left. Some water inefficiently interacts with the blades due to edge effects and deviation of the jet's entrance angle from the no-shock condition. Clearly, the number of blades interacting with the flow will affect the turbine's performance.

In the following sections, the interaction terms in Equation (18) are explored. Throughout the analysis, d/D is replaced with d for simplicity; the results are equivalent.

α and Z

According to Equation (19), α_{opt} scales with Z, which means that as the number of blades increases and the other parameters remain constant, the incident angle of the nozzle should increase to maintain optimum performance. Surface plots are used to illustrate this interaction between α and Z. In Fig. 14, α and d are plotted against efficiency and three plots are overlaid, each corresponding to a different Z. As Z increases, α_{opt} shifts to the right. Furthermore, the turbine's efficiency is at its lowest when there are few blades and a large incident angle. This suggests that the number of blades, as seen from the cross-sectional viewpoint of the jet, is important to fully capturing the water. The greater the angle, the more space there is for water to flow unimpeded. The converse is also true by Equation (20): Z_{opt} scales with α.

In general, the turbine is mostly unaffected by misalignments in α. Under most circumstances, if α strays 10° in either direction of α_{opt}, the turbine's efficiency can be expected to drop by only 2%.

Fig. 13. Photo of water splitting between two blades.

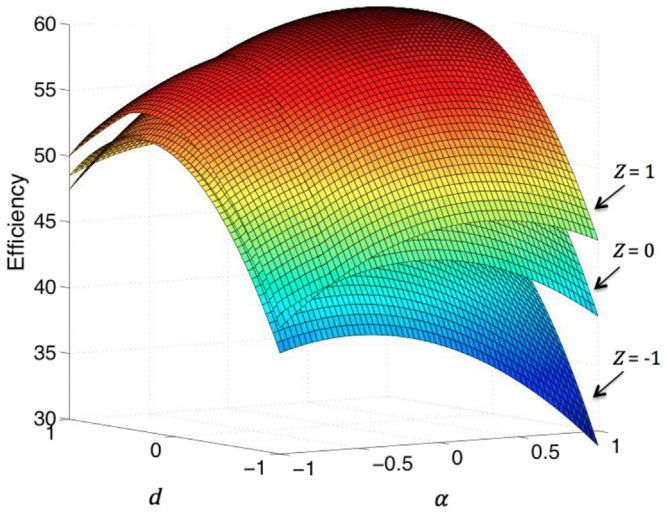

Fig. 14. Jet angle (α) and nozzle diameter (d) with blade number (Z) overlaid. $\varphi = 0$.

d and Z

In comparison to previous literature, Equation (20) is the Turgo equivalent to Tygun's formula for the Pelton turbine, shown by Equation (9), verifying that the number of blades impacts the Turgo's efficiency and that the optimum number of blades depends on α, d and φ. Equations (20) and (21) indicate that the optimum blade number and nozzle diameter are inversely related to each other; however, Figs. 14 and 15 show that this interaction is minimal. For example, increasing the nozzle diameter from 7 mm to 19 mm results in only a slight decrease in the optimum number of blades (Fig. 15). Conversely, doubling the number of blades from 10 to 20 results in a slight decrease in the optimum nozzle diameter (Fig. 14).

This is not to say that the ratio of nozzle diameter to blade spacing, d/s (spacing, s, is just the reciprocal of Z multiplied by the turbine's circumference, a constant), is not important (see section 3.4); indeed, it is. In Fig. 14, for $\alpha = 25°$, a 7 mm nozzle with 10 blades ($d/s = 0.17$) has an efficiency of 37%, while the same nozzle with 20 blades ($d/s = 0.35$) is 46% efficient. Furthermore, a 19 mm nozzle with 20 blades ($d/s = 0.91$) yields an efficiency of 56%. In Fig. 16, efficiency versus d/s ratio is plotted for every trial. The trend suggests that there must be a sufficient number of blades ($d/$

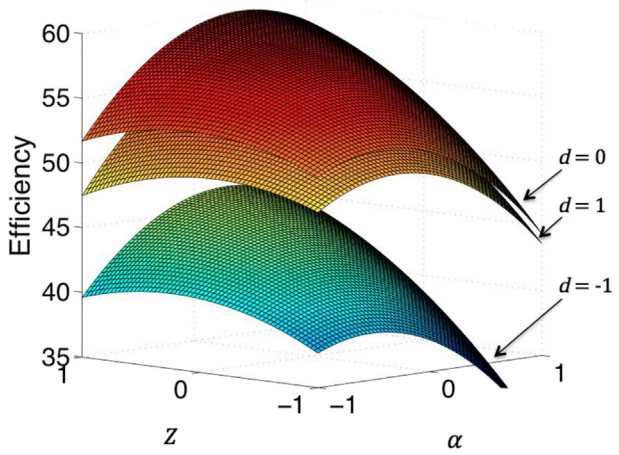

Fig. 15. Jet angle (α) and blade number (Z) with nozzle diameter (d) overlaid. $\varphi = 0$.

$s > 0.45$) in order to fully capture and reverse the flow of water.

There is a large spread in efficiencies for each value of d/s because each turbine speed is plotted ($\varphi = 0.25$, 0.35 and 0.45). In reality, once d/s is set by site characteristics and turbine design, a turbine operator has the flexibility to fine-tune φ to the BEP. Therefore, for each d/s ratio tested, the efficiency that corresponds to the experimental BEP (the peak in Fig. 12, for example) is plotted in Fig. 17.

α and d

Recalling Section 3.1, theory states that α_{opt} is a function of φ and β_2 only. From Equation (19), it is clear that the optimum inlet angle also depends on the number of blades and the nozzle diameter. Equation (19) also confirms Williamson's findings, which indicate that α_{opt} scales with d. If the nozzle diameter increases, the incident angle of the nozzle should increase as well. The converse is also true: d_{opt} scales with α, as shown by Equation (21).

While the interaction between α_{opt} and d is statistically significant, Fig. 15 shows that α_{opt} remains relatively unchanged. At $Z = 10$, a change from a 7 mm–19 mm nozzle correlates to α_{opt} increasing from 16.8° to 20.1°, not nearly as substantial as the 10° shift observed by Williamson. In this sense, while the trends are similar, the results of the UC Davis turbine indicate that the optimum jet inlet angle is much less sensitive to changes in nozzle diameter.

Moreover, Massey [18] states that α_{opt} is generally a few degrees less than $\alpha_{no\text{-}shock}$. For the spoon's inlet angle of 79°, a theoretical calculation gives $\alpha_{no\text{-}shock}$ to be 42°, so the experimental values of $\alpha_{opt} = 35°$ is in agreement with Massey.

α and φ; d and Z

Equations (19) and (22) show that α and φ are inversely related to each other. Fig. 18 shows that at higher speeds, the turbine performs best with a small jet angle and as the speed decreases, α_{opt} increases. Conversely, by Equation (22), the smaller the jet angle, the larger φ_{opt} will be. This is because at small jet angles the velocity vector, $v \cos \alpha$, will be larger, requiring the turbine to spin faster in order for all the water to be captured. Equation (22) also highlights that Z and d affect φ_{opt}, and not just α and β_2, as described in Section 3.2.

φ and Z

Fig. 18 also highlights a major interaction between Z and φ. At fast turbine speeds more blades are necessary. For example, at $\varphi = 0.45$ and $\alpha = 25°$, the turbine with 10 blades is 45.5% efficient and with 20 blades it is 59.0% efficient. At slow turbine speeds whether fewer blades are necessary depends on the value of α.

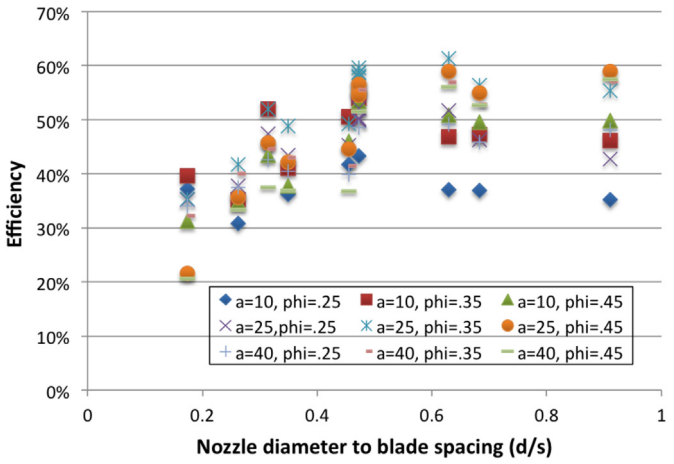

Fig. 16. Effect of nozzle diameter to blade spacing ratio on efficiency.

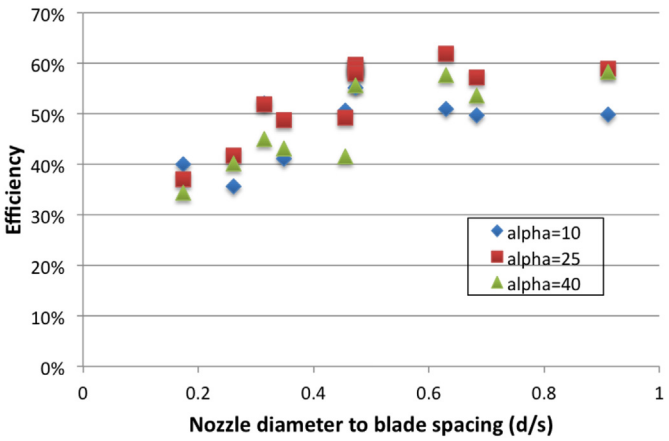

Fig. 17. Nozzle diameter to blade spacing ratio – Best Efficiency Points only.

5.5. Effect of axial impact location on efficiency

Three levels of axial impact location were tested. The locations were −8 mm (toward the leading edge), 0 mm (the center of the blade), and 8 mm (toward the discharge edge). Three replicates were collected at each level. A Tukey multiple comparison test was performed and the analysis revealed that 8 mm and 0 mm are not significantly different from each other, but that −8 mm was slightly lower in efficiency (Fig. 19). The impact location affects the performance of the UC Davis turbine by only a couple of percentage points, making it relatively robust against misalignment of the jet's axial impact location.

5.6. Effect of blade orientation angle on efficiency

The purpose of this experiment was to understand the turbine's sensitivity to changing the blade's orientation angle and to find the best orientation angle. As stated in Section 3.2, the discharge angle, β_2, is typically set to 15–20° to prevent effluent water from interfering with the oncoming blade. However, in this experiment, to change the discharge angle, the blade's orientation angle had to be changed because the curvature of the spoon was constant. Therefore, the experiment cannot distinguish whether an effect is due to

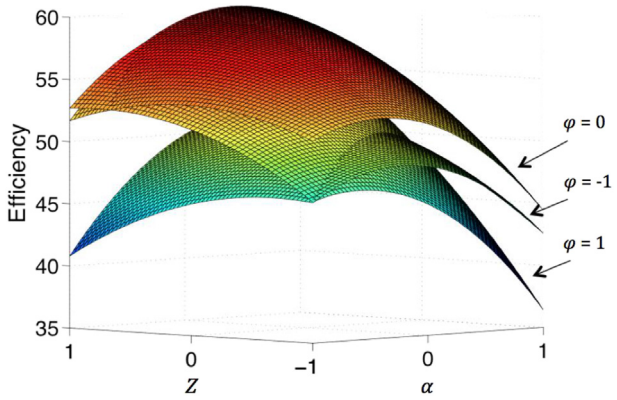

Fig. 18. Jet angle (α) and blade number (Z) with speed ratio (φ) overlaid. $d = 0$.

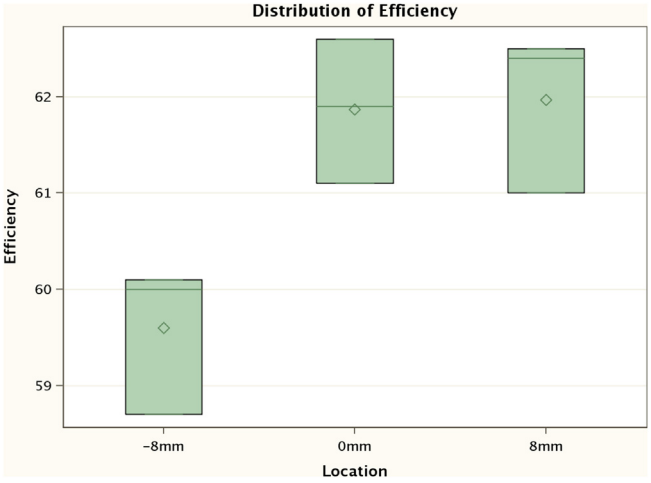

Fig. 19. Box plot of efficiency versus the jet's axial impact location.

the discharge angle or the blade's inlet angle, only the orientation angle. Discharge angle is only used for reference.

The orientation angle, which was held constant at 30° for the Central Composite Design experiment, was also tested at 25°, 35°, and 40°. The equivalent discharge angles were 9°, 15°, 19° and 24°. The jet inlet angle was kept constant at 30°. Three replicates were performed at each level, and for each experiment the peak efficiency and the corresponding best operating speed ratio were recorded as response variables.

First, a box plot of efficiency versus discharge angle is shown in Fig. 20. While the discharge angle appears to have a parabolic trend that peaks in efficiency near 19°, Duncan and Tukey tests indicate that angles 14°, 19° and 24° are not significantly different from each other at a 95% confidence level.

Secondly, the best operating speed ratios for each discharge angle are plotted in Fig. 21 and a Duncan Multiple Range test confirms that the values of φ are significantly different from each other. The best operating speed ratio decreases linearly with increasing discharge angle, which is what theory predicts, except the experimental φ_{opt} is smaller and has a greater slope (see Table 6). The theoretical calculations assume a friction factor of $k = 0.9$. In reality, the friction factor should be larger for this turbine, accounting for the discrepancy between experiment and theory.

In summary, a blade discharge angle of 19° is recommended. Straying from this angle by ±5° does not result in any significant change in turbine efficiency, but will affect the best operating speed ratio slightly.

6. Conclusions and future work

Using a face-centered central composite experiment, a regression equation was developed to predict the efficiency of a low-cost Turgo turbine as a function of jet inlet angle, number of blades, nozzle diameter, and the rotational speed of the turbine. Significant second-order effects were noticed. The nozzle diameter and the turbine's speed ratio played the most prominent roles in influencing the turbine's efficiency, as did the interaction between jet angle and number of blades, number of blades and speed ratio, and nozzle diameter and speed ratio. The prediction equation had an R^2_{adj} equal to 0.93, indicating that the second order model is sufficient and that higher order terms would not likely improve the model.

Due to the second order nature of the prediction equation, a global optimum point was calculated. The optimum jet angle was 35°, or 7° less than the no-shock angle, which is relatively large due to the spoons' shallow curvature compared to typical turgo blades. The optimum speed ratio was 0.425, the optimum number of blades was 25, and the optimum jet diameter was 15.4 mm, which corresponds to a ratio of $d/s = 0.94$ These optimum values will vary based on a site's head and flow, but the optimization equations developed in this study enable the designer to calculate the best values of α, Z, d and φ.

Of particular interest, the equation for optimum jet angle depends heavily on the number of blades, moderately on the speed ratio, and slightly on the nozzle diameter. The results also indicate that the turbine performs best when the ratio d/s is greater than 0.45. Furthermore, the results indicate that variations in the jet's axial impact location on the blade and the blade's orientation angle do not severely degrade the turbine's performance. The turbine performed the best when the jet was aimed at the center of the blade and at an orientation of about 30°.

This particular tablespoon turbine could be a more economical alternative to off-grid villages than hydroelectric turbines that require casting and pattern-made molds or that are purchased commercially and imported. The turbine's materials, including shaft and bearings, were locally available and repurposed and the

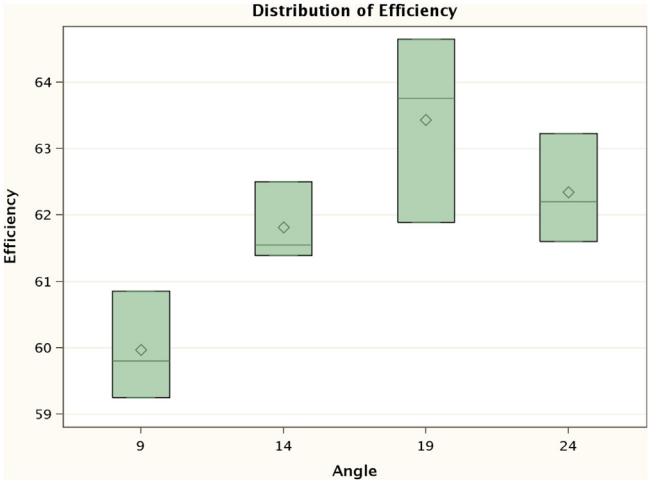

Fig. 20. Plot of efficiency versus blade discharge angle.

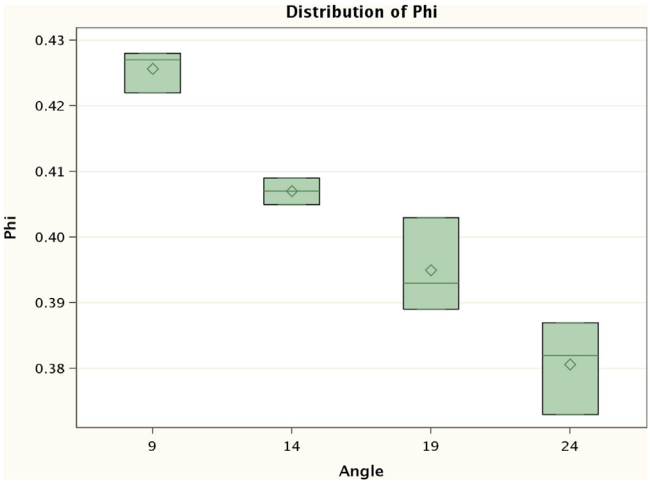

Fig. 21. Speed ratio versus blade discharge angle.

Table 6
Experimental and theoretical comparison of the effect of discharge angle on efficiency and speed ratio.

Orientation angle	Discharge angle[a]	Actual efficiency	Theoretical efficiency	Experimental φ_{opt}	Theoretical φ_{opt}
25°	9°	60%	92.6%	0.425	0.563
30°	14°	61.8%	91.6%	0.408	0.561
35°	19°	63.4%	90.2%	0.395	0.558
40°	24°	62.4%	88.2%	0.381	0.555

[a] For reference only; discharge angle is not necessarily responsible for effects on the efficiency or φ_{opt} because the blade inlet angle also changed.

cost of new parts totaled to $35. Furthermore, the design guidelines produced by this study can be used to rapidly design commercial Turgo Turbines with geometrically similar blades for a specific site's head and flow, thereby improving mechanical efficiency.

Acknowledgments

We are grateful for the help of those at the UC Davis Utilities, the UC Davis Blum Center for Developing Economies and the UC Davis D-Lab. Special acknowledgement to Christophe Nziyonsenga in Rwanda and undergraduate researchers Terence Hong, Roger LeMesurier, Yuka Matsuyama, and Kevin Wong for their assistance.

References

[1] M. Maloney, Energy recovery from public water systems, Water Power Dam Constr. (2010 July) 18–19.
[2] A.A. Lahimer, M.A. Alghoul, K. Sopian, N. Amin, N. Asim, M.I. Fadhel, Research and development aspects of pico-hydro power, Renew. Sustain. Energy Rev. 16 (8) (2012) 5861–5878.
[3] A.A. Williams, R. Simpson, Pico hydro – reducing technical risks for rural electrification, Renew. Energy 34 (8) (2009) 1986–1991.
[4] S. Mishra, S.K. Singal, D.K. Khatod, Optimal installation of small hydropower plant—a review, Renew. Sustain. Energy Rev. 15 (8) (2011) 3862–3869.
[5] M. Pigaht, R.J. van der Plas, Innovative private micro-hydro power development in Rwanda, Energy Policy 37 (11) (2009) 4753–4760.
[6] T. Meier, G. Fischer, Assessment of the Pico and Micro-hydropower Market in Rwanda, Entec AG, 2011 December (Report No.).
[7] L. Kosnik, The potential for small scale hydropower development in the US, Energy Policy 38 (10) (2010) 5512–5519.
[8] Home Power Systems (cited 2013 August 23); Available from: http://www.homepower.ca/dc_hydro.htm.
[9] D. Ledbetter, E. Orlofsky. The Harris hydroelectric system. (cited 2013 August 9); Available from: http://harrishydro.biz/.
[10] N. Smith, G. Ranjitkar, Nepal Case Study – Part One: Installation and Performance of the Pico Power Pack, The Nottingham Trent University, Nottingham, UK, 2000, p. 3.
[11] S.D.B. Taylor, M. Fuentes, J. Green, K. Rai, Stimulating the Market for Pico-hydro in Ecuador, IT Power, Hampshire, UK, 2003.
[12] E.S. Design, Stream Engine, 2011 (cited 2013 August 9); Available from: http://www.microhydropower.com/our-products/stream-engine/.
[13] J. Hartvigsen, Hartvigsen-hydro Components for Microhydro Systems, 2012. Available from: http://www.h-hydro.com.
[14] B.R. Cobb, K.V. Sharp, Impulse (Turgo and Pelton) turbine performance characteristics and their impact on pico-hydro installations, Renew. Energy 50 (2013) 959–964.
[15] P.N. Wilson, A high-speed impulse turbine, Water Power (1967) 25–29.
[16] S.J. Williamson, B.H. Stark, J.D. Booker, Performance of a low-head pico-hydro Turgo turbine, Appl. Energy 102 (2013) 1114–1126.
[17] A.H. Gibson, Hydraulics and its Applications, Constable & Company, London, 1954.
[18] B. Massey, J. Ward-Smith, Mechanics of Fluids, eighth ed., Taylor & Francis, New York, 2006.
[19] P. Fraenkel, O. Paish, V. Bokalders, A. Harvey, A. Brown, R. Edwards, Micro-hydro Power: a Guide for Development Workers, IT Publications, London, 1999.
[20] B.R. Cobb, Experimental Study of Impulse Turbines and Permanent Magnet Alternators for Pico-hydropower Generation, Oregon State University, 2012.
[21] J.S. Anagnostopoulos, D.E. Papantonis, Flow modeling and runner design optimization in turgo water turbines, World Acad. Sci. Eng. Technol. 22 (2007) 207–211.
[22] P. Maher, N. Smith, Pico Hydro for Village Power, 2001.
[23] A. Harvey, Micro Hydro Design Manual, Intermediate Technology Publications, London, 1993.
[24] P.K. Koukouvinis, J.S. Anagnostopoulos, D.E. Papantonis, SPH method used for flow predictions at a Turgo impulse turbine: comparison with fluent, World Acad. Sci. Eng. Technol. 79 (2011) 659–666.
[25] S.A. Korpela, Principles of Turbomachinary, Wiley, Hoboken, New Jersey, 2011.
[26] J.M. Cimbala, Essentals of Fluid Mechanics: Fundamentals and Applications, McGraw-Hill, Europe, 2007.
[27] J. Thake, The Micro-hydro Pelton Turbine Manual: Design, Manufacture and Installation for Small-scale Hydro-power, ITDG Publishing, 2000.
[28] C. Cornaro, A.S. Fleischer, R.J. Goldstein, Flow visualization of a round jet impinging on cylindrical surfaces, Exp. Therm. Fluid Sci. 20 (2) (1999) 66–78.
[29] V. Kadambi, M. Prasad, An Introduction to Energy Conversion, John Wiley & Sons, 1977.
[30] G. Biswas, S. Sarkar, S.K. Som. Fluid Machinery. (cited 2013 August 10); Available from: Nptel.iitm.ac.in/courses/Webcourse-contents/IIT-KANPUR/machine/ui/TOC.htm.
[31] S.J. Williamson, B.H. Stark, J.D. Booker, Low head pico hydro turbine selection using a multi-criteria analysis, Renew. Energy 61 (2014) 43–50.
[32] M. Nechleba, Hydraulic Turbines: Their Design and Equipment, Constable & Co, London, 1957.
[33] J.S. Gulliver, R.E. Arndt, Hydropower Engineering Handbook, Mcgraw-Hill, 1990.
[34] P. Singh, F. Nestmann, Experimental investigation of the influence of blade height and blade number on the performance of low head axial flow turbines, Renew. Energy 36 (1) (2011) 272–281.
[35] M. Murakami, K. Katayama, Discharge coefficients of fire nozzles, J. Basic Eng. 88 (4) (1966) 706.
[36] S. Shafii, S.K. Upadhyaya, R.E. Garrett, The importance of experimental design to the development of empirical prediction equations, Trans. ASAE 39 (2) (1996) 377–384.
[37] M. Islam, L.M. Lye, Combined use of dimensional analysis and statistical design of experiment methodologies in hydrodynamics experiments, in: 8th Canadian Marine Hydromechancis and Structures Conference; Newfoundland, Canada, 2007.
[38] D.D. Gray, A First Course in Fluid Mechanics for Civil Engineers, Water Resources Pubns, 2000, p. 487.
[39] D. Rubinstein, S.K. Upadhyaya, M. Sime, Determination of in-situ engineering properties of soil using response surface methodology, J. Terramechanics 31 (2) (1994) 67–92.
[40] M. Kutner, C. Nachsheim, J. Neter, W. Li, Applied Linear Statistical Models, McGraw-Hill, New York, 2005.